



The Locust antenna as an odor discriminator

Shvil Neta^a, Golan Ariel^b, Yovel Yossi^{a,c,d,***}, Ayali Amir^{a,c,**}, Maoz M. Ben^{a,b,e,*}

^a Sagol School of Neuroscience, Tel Aviv University, Tel Aviv, Israel

^b Department of Biomedical Engineering, Tel Aviv University, Tel Aviv, Israel

^c School of Zoology, Tel Aviv University, Tel Aviv, Israel

^d School of Mechanical Engineering, Tel Aviv University, Tel Aviv, Israel

^e The Center for Nanoscience and Nanotechnology, Tel Aviv University, Tel Aviv, Israel



ARTICLE INFO

Keywords:

Biosensors
Insects olfaction
Odor-discrimination
Electroantennogram
Machine-learning
Bio-hybrid systems

ABSTRACT

Identifying chemical odors rapidly and accurately is critical in a variety of fields. Due to the limited human sense of smell, much effort has been dedicated to the development of electronic sensing devices. Despite some recent progress, such devices are still no match for the capabilities of biological (animal) olfactory sensors, which are light, robust, versatile, and sensitive. Consequently, scientists are turning to a new approach: Bio-Hybrid sensors. These sensors combine animal biological sensors with electronic components to achieve maximum detection and classification while conveying a comprehensible signal to the end user.

In this work, we created a bio-hybrid odor discriminator utilizing the desert locust's primary olfactory apparatus - its antennae, together with simple electroantennogram technology and artificial intelligence tools for signal analysis. Our discriminator is able to differentiate between at least eight pure odors and two mixtures of different odorants, independently of odorant concentration. With four orders of magnitude higher sensitivity than gas chromatography-mass spectrometry, it is able to detect the presence of less than 1 ng of volatile compounds and, compared to other bio-hybrid sensors available today, it can be easily operated by an unskilled individual. This study thus opens up the future for robust and simple bio-hybrid robotic sensing devices that can be widely deployed.

1. Introduction

Identifying hazardous chemical leaks, detecting explosives and drugs in airports, and preventing the distribution and consumption of spoiled food are just some examples of the importance of fast and accurate identification of various odors (Saha et al., 2020). Unfortunately, the human sense of smell is inadequate to provide a suitable solution to most of these challenges. Consequently, various artificial olfaction devices have been proposed and devised. Most of the existing odor-detection devices, also known as electronic noses (e-noses), focus on identifying the volatile molecules that compose the odor through recognition of their structure, mass/charge ratio, conductivity, light transition, etc., using a pattern-recognition engine (Chen et al., 2022; Larisika et al., 2015; Latif et al., 2016). Despite proving some efficiency in recognizing odors (Skarysz et al., 2018), and even in diagnosing a variety of diseases via the breath (Nakhleh et al., 2017), those sensors, in addition to being

high-maintenance and high-cost, are still inferior to their biological (animal) counterparts in robustness, sensitivity, size, response time, precision, and simplicity (Supp. Table 1) (Shor et al., 2020; Vouloulsi et al., 2015).

Consequently, harnessing nature to their aid, scientists are seeking to incorporate animals' sensory organs into effective odor-detection and discrimination devices. Among the different biological sensors, the integration of insect sensors is often a preferred choice (Fishel et al., 2021; Kuwana et al., 1999; Martinez et al., 2014; Myrick et al., 2008) as these are usually easy to dissect, small, lightweight, and energetically efficient, while also excelling in sensitivity and robustness. In respect to sensitivity, for example, a male moth can detect the female pheromone (Bombykol) at amounts as low as $3 \cdot 10^{-6}$ µg (Kaissling and Priesner, 1970), while the locust was reported to detect odors in concentrations of less than 1 ppb (Saha et al., 2020). In this study, we utilized the antennae (the main olfactory apparatus) of the desert locust (*Schistocerca gregaria*)

* Corresponding author. Sagol School of Neuroscience, Tel Aviv University, Tel Aviv, Israel.

** Corresponding author. Sagol School of Neuroscience, Tel Aviv University, Tel Aviv, Israel.

*** Corresponding author. Sagol School of Neuroscience, Tel Aviv University, Tel Aviv, Israel.

E-mail addresses: yossiyovel@gmail.com (Y. Yossi), ayali@tauex.tau.ac.il (A. Amir), bmaoz@tauex.tau.ac.il (M.M. Ben).

as a model to address the challenging task of odor identification and discrimination (Fig. 1A and B).

The locust antenna comprises more than 50,000 olfactory receptor neurons (ORNs) that convert airborne odorant molecules into electrical signals (Raman et al., 2010; Saha et al., 2013a). There are several methods for recording the insect's physiological response to volatiles, based on measuring electrical signals from the different parts of the olfactory system. At the single ORNs level, one can record the electrical potentials from a single sensillum (pl. sensilla) (Jacob, 2018; Olsson and Hansson, 2013), (Fig. 1C) containing one to a few ORNs each. At the central nervous system (brain) level, one can insert electrodes and record the downstream electrophysiological activity from the antennal

lobe (AL). In between these two levels lies the antenna and the electroantennogram (EAG) (Ep-a et al., 2007; Olsson and Hansson, 2013), which measure the odorant-induced combined extracellular potential changes of the ORNs reflected in the potential difference between the two ends of the antenna (Raman et al., 2010).

While the two former methods (single sensillum and AL recording) can provide very detailed information, they usually require expensive equipment, highly skilled operators, and complex signal analysis. In AL recordings, for example, the neuronal firing patterns and their dynamics are highly dependent on multiple factors, including environmental conditions (Nizampatnam et al., 2021), the presence of background odors (Haney et al., 2018; Saha et al., 2013b), stimulus history (Mallik

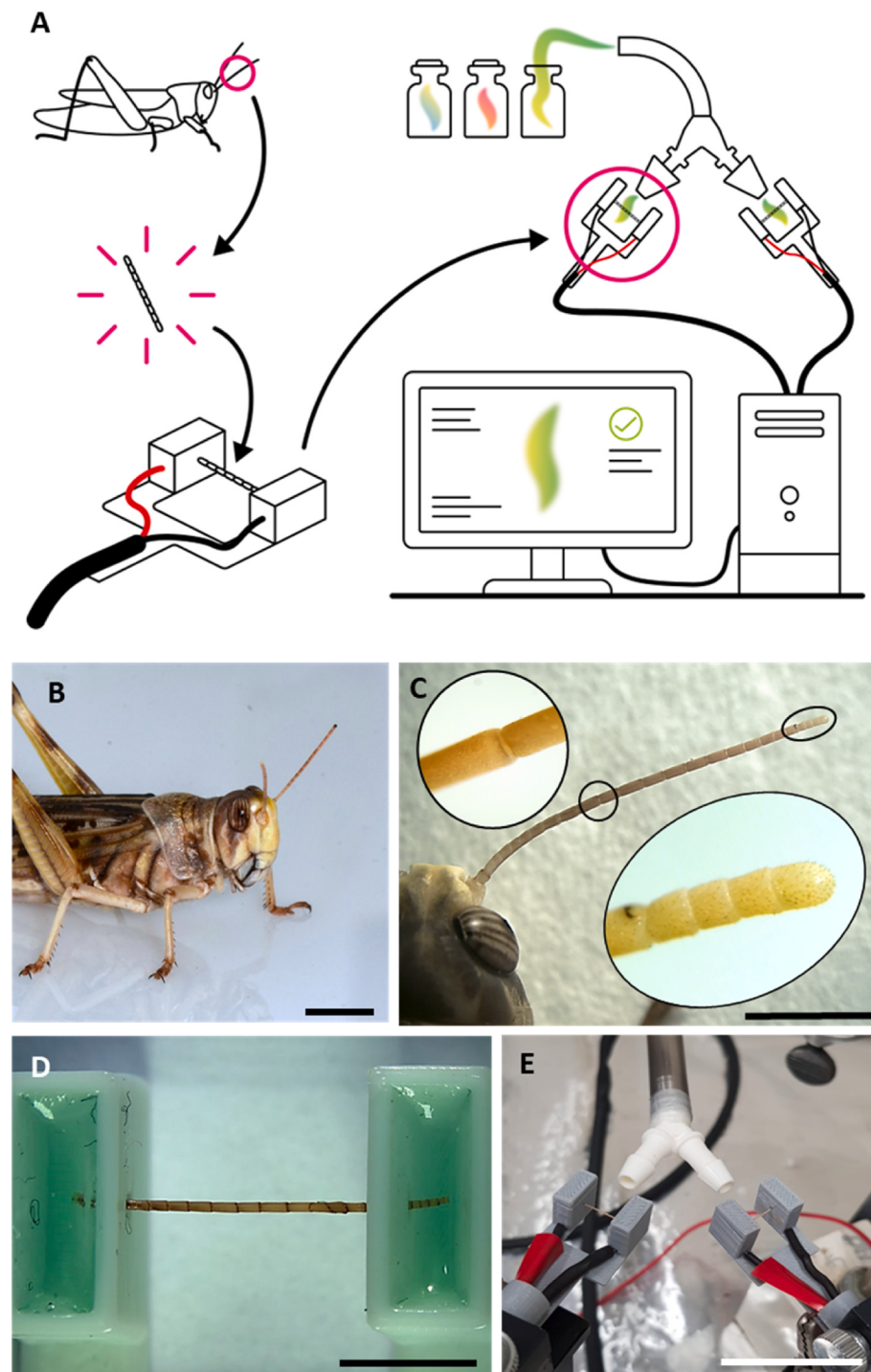


Fig. 1. Recording the locust olfactory system. (A) The construction of an odor discriminator using the locust antennae. (B) The primary organ for sensing chemical compounds in the desert locust. (C) The antennae are covered by hair-like appendage structures. Scale bar: 1 cm and 0.5 cm, in B and C respectively. (D) An excised antenna in the conductive gel-filled antenna holder, scale bar 0.5 cm. (E) The recording set-up shows the double nozzle for introducing the odorants, and two sets of electrodes inserted into two holders for simultaneous two-channel recordings. scale bar 2.5 cm.

et al., 2020; Nizampatnam et al., 2018; Renou and Anton, 2020), concentration (Raman et al., 2010), and electrode location in the brain (which neurons are being recorded), which may cause high variability and limited reproducibility.

EAG, in contrast, is simple to construct and use, and significantly less expensive. The measured signal, however, offers relatively limited information and, to the best of our knowledge, there are no reports to date of successfully utilizing EAG from a single antenna to discriminate one volatile compound from another. This limitation mostly results from the summed ORNs population activity concealing the diversity in the individual ORN's odor-specific temporal response (Raman et al., 2010), and also from the concentration-dependent response. In order to discriminate between odors using EAG, previous research, therefore, turned to compare the response spectra of at least two different insect species (Myrick et al., 2009, 2008).

Here we present a bio-hybrid odor discriminator using EAG measurements from a single locust antenna and a machine learning-based algorithm. We were able to successfully identify and discriminate single odors, independent of their concentration, when presented in isolation, as well as in odor mixtures.

2. Materials and methods

2.1. Animals

Young adult male desert locusts (*Schistocerca gregaria*) from our breeding colony at the School of Zoology, Tel Aviv University were used in all experiments. The locusts were reared over many generations in 60-Liter metal cages at a density of 100–160 insects per cage, under controlled conditions of 30 °C, 35–60% humidity, and a 12D:12 L cycle. Additional radiant heat was provided by 25 W incandescent electric bulbs during the daytime, to reach a final day temperature of 35–37 °C. The locusts were fed wheat seedlings and dry oats daily. All experiments followed the institutional regulations for work with invertebrate animals.

2.2. The electroantennogram recordings and antenna holder design

The antenna was removed from the locust, its distal end was trimmed, and it was mounted in the custom-constructed antenna holder.

An inherent challenge in EAG recordings is the relatively low signal-to-noise ratio. To tackle this, we developed an antenna holder (Fig. S1D), in which the antennae tips are not in direct contact with the electrodes, but are rather submerged in (i.e., they interact via) conductive gel-filled chambers (Sigma Gel, Parker), as shown in Fig. 1D. The new design allowed recordings that were less noisy and more stable compared to the “standard”, commonly used, electrode holders (Fig. S1E). Moreover, it reduces vibration-induced noise, as the gel acts as a shock absorber/suspension system. The antenna holder was designed using SolidWorks® (SolidWorks, Corporation, MA) and printed using a Raise 3D Pro2 Dual Extruder 3D Printer (Raise Technologies, Inc.).

The two ends of the antenna were inserted into the middle of each compartment, through two holes drilled in the walls (Fig. 1D, S1D). Tightly-fitting lids were added to the two compartments to reduce gel evaporation (Fig. 1E) enabling us to keep the antenna functional up to 11 h (Response to an odor was detected even after 11 h compared to ~2–3 h in the literature, Fig. 2S (Martinez et al., 2014; Schott et al., 2013)).

The EAG system for recording the odor-induced signals (Fig. S1A) comprised: (1) two antenna holders and electrode sets (Silver electrodes, 0.025" Bare, 0.030" coated, PFA silver (Ag), A-M Systems, Sequim WA), (2) four-channel differential AC amplifiers (Model 1700, A-M Systems, Bellevue, WA, USA), (3) a 2-channel signal acquisition interface IDAC-2 (SYNTECH, Hilversum, The Netherlands), and, (4) a PC with EAGPro software or Auto-Spike software (SYNTECH, Germany). Signals were amplified (100 times), filtered (1 Hz-HPF/500 Hz-LPF) and then

sampled at 100 Hz to a PC.

In addition, we developed a “Y” shaped tube at the tip of the EAG system (Fig. 1E, Fig. S1F), which enables the simultaneous recording of two experiments (using two separate channels). In addition to increasing the system's throughput, it enables the comparison of different conditions and increases the robustness of the system (for example left and right antennae of the same locust).

2.3. The odorants

A 5 µl sample of the odorant of interest was applied on a thin strip of filter paper (Whatman #5, WHATMAN LIMITED, England), and inserted into a short Pasteur pipette (glass, 15 mm, witeg, Germany). The pipette was attached to a stimulus controller (CS-55, SYNTECH, Germany) at one end, and to an aluminum mixing tube at 45°, at the other. (Fig. S1A). An odor stimulation was applied via a pedal press, using the stimulus controller. Each stimulus was applied in 3 repetitions at 1-min intervals.

The odorants used in the experiments were Benzaldehyde, β-Citronellol, 1-Hexanol, Geraniol and Ethyl-Butyrate (all from Sigma-Aldrich) diluted to 93 mM unless stated otherwise (see results) in mineral oil (Sigma-Aldrich). Lemon and rosemary oils and vanilla extracts (from a health shop). Mineral oil was also used as a blank control in all trials.

For the mixture experiments, equal amounts of both odorants were added to the mixture to reach a final concentration of 93 mM (similar to that in the single odor experiments).

2.4. Gas chromatography–mass spectrometry

Benzaldehyde quantitates were estimated by Solid Phase Micro-extraction (SPME) sampling followed by thermal desorption into GC-MS inlet and further analysis. We assume similar quantities of compounds of interest accumulated on both the locust antenna and the SPME fiber. This is based on similar dimensions and comparable experimental setup. The SPME fiber (100µm PDMS, 24 Ga, Supelco PN: 57300-U, Sigma Israel) was exposed to a 0.5 s stimulus pulse and retracted 5 s after stimulus termination. Immediately after, it was manually inserted into the GC-MS inlet where it was thermally desorbed.

Compounds identities were validated by comparison to NIST Mass Spectral Library (Version 2.0, 2012 NIST) (Figs. S4C and D). The Benzaldehyde quantities were calculated by injecting benzaldehyde standard solutions at the same GC-MS conditions as the SPME analysis and then comparing the instrument's response (chromatographic peak area) to the calibration curve (Fig. S5A). Standard solutions were prepared by subsequent dilutions of the stock solution (2000 ng/µl benzaldehyde in n-hexane).

2.5. Data analysis

The recordings were analyzed as follows: Each condition (control/odor type/concentration/stimulus duration/antenna part) was repeated in triplets (three repeats for each antenna). The three blank control repetitions for each antenna were averaged and the average was deducted from the recordings obtained in the corresponding experiment. The median offset was applied to each repetition (after subtracting the blank response) separately and, finally, the average of all repetitions of the same condition was computed and plotted using Prism (GraphPad Prism 8.0.1).

Processing was performed in Python3 (Python Software Foundation, Scotts Valley, CA) accompanied with the Graphical User Interface. The code performs the necessary calculations noted above and provides a graphical interface for visualization of the data, as well as organizing and exporting the data in a format suitable for Excel and Prism. (Fig. S1B&C).

2.6. Comparing the left and right antennal responses

We examined whether both of the locust's antennae (left and right) provided a similar response to odorants, as different responses may bias the algorithm results and it is known that some insects display differences between their two antennae (Lockett and Willis, 2015; Rogers et al., 2013). To examine this, we compared the amplitude and shape of the EAG response of the left and the right antenna to various odorants.

In order to compare the left and right antennal response amplitude, we substituted the post-analysis minimum voltage value for each repetition in the following equation (E.q.1):

$$(IRI - ILI) / (IRI + ILI) \quad (1)$$

* R = Right antenna, L = Left antenna

As Fig. S3A, B&C shows, there was no significant difference in the response between the left and right antenna of the same locust (ns in Wilcoxon test, see methods). These results enabled us to use the data from the left and right antennae in the same train and test groups, as carried out throughout this work.

2.7. Machine-learning classifier

We used a random forest classifier for odor classification, written in Python3 (Python Software Foundation, Scotts Valley, CA). The input to the classifier was the first 1500 ms of the EAG normalized time signal, recorded at 100 Hz. When preprocessing the data, each analyzed repetition's minimum point (after blank and offset deduction (See data analysis) was normalized to a minimum of [-1]. The database was then split into 'train' and 'test' sets using a 'Leave-one-group-out' paradigm (unless stated otherwise), where each antenna was categorized as a separate group and all recordings from a single antenna were thus used as the test set for all other recordings (Fig. S4A). This procedure ensured that repetitions from the same antenna were not used in both the train and the test pool. We used the balanced accuracy to report performance.

2.8. Statistics

To test the significance of the classifier's results we used a two-tailed binomial test, where chance was defined according to the number of

classes and N was the number of antennae in each experiment (Suppl. Table 2). For the left and right comparison, we used a one-sample t and Wilcoxon test.

3. Results

3.1. Different odorants induce unique EAG responses

The antennal response to different odors demonstrated a unique EAG profile for each of the eight specific odorants tested (Fig. 2A&B), which was also consistent across the various concentrations tested (Fig. 3A&B). A random-forest algorithm was able to identify and discriminate the eight odorants based on the electrophysiological signal, at high rates, with a balanced accuracy of 69.3%, significantly exceeding chance (12.5%, Fig. 2C, P < 0.0001). Additionally, as a control for over-fitting, we shuffled the labels of the original data file, and trained the algorithm again. In this case, the balanced accuracy was 12.0%, which is close to the random probability (12.5%, the difference was non-significant (ns) in a binomial test) (Fig. S4B).

The eight odorants could be roughly divided into three groups based on the superficial resemblance of their EAG responses (Fig. 2B) (Hallem and Carlson, 2006). To examine the ability of our system to discriminate between closely-related odors, we trained the algorithm to identify an odorant within a specific group. As shown in Figs. S4C and D & E, the algorithm was able to distinguish the odorants more accurately than random (33% for three odorant and 50% for two), with 85.1% accuracy for Benzaldehyde, 1-Hexanol, and Ethyl-butrate (Fig. S4C, P < 0.0001), 65.4% accuracy for β -citronellol, Geraniol and Lemon (Fig. S4D, P < 0.0001), and 74.6% accuracy for Lemon and Rosemary (Fig. S4E, P = 0.01).

3.2. Different odor concentrations

Fig. 3A and B presents the EAG signal for two randomly chosen odorants at different concentrations (different dilutions). As can be seen, the EAG signal corresponds to the relative concentration of the odorant, and the odorant could be still detected and identified at a concentration nine orders of magnitude lower than the initially introduced concentration (93 mM, Fig. 3A–D).

In order to test the odor-discriminator detection limits in terms of absolute quantities rather than relative concentrations, we placed a

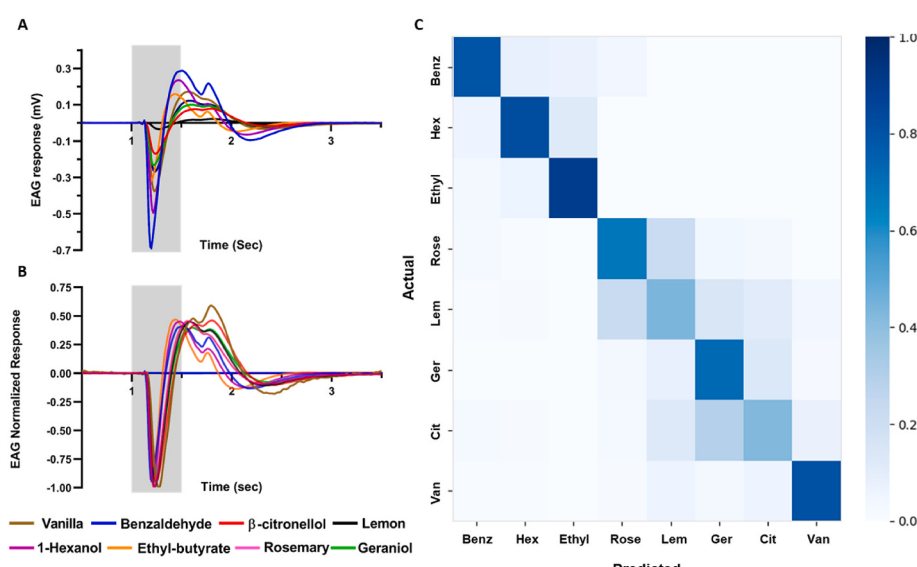


Fig. 2. Different odorants generate distinct response profiles. (A) Response profiles of the locust antenna to different odors, all at the same concentration (93 mM), N = 17–22 Locusts, 31–42 antennae, 93–126 repetitions. (B) The response profiles from A with the most negative point normalized to -1. In both A and B, the duration of the stimulus is shaded gray. (C) Confusion matrix calculated for the odorant responses shown in B, with an average accuracy of 69.34% for 972 samples.

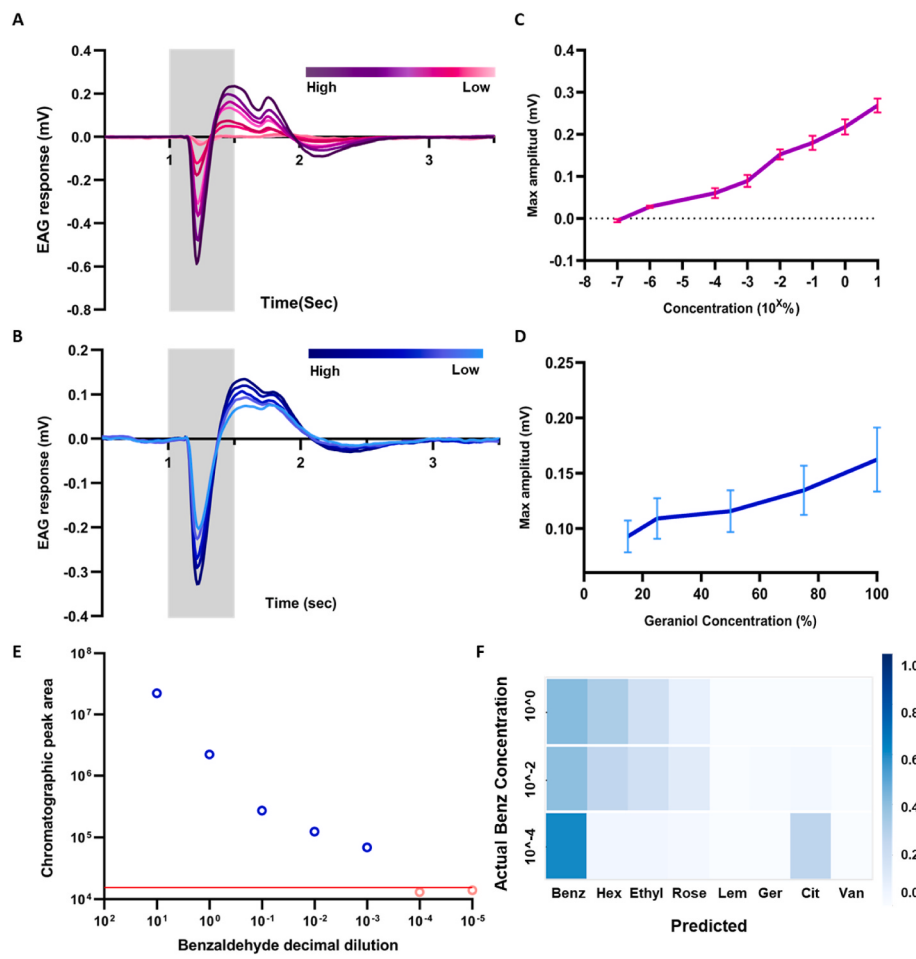


Fig. 3. The effect of odorant concentration on the discrimination capacity. (A) Response profiles of the locust antenna to different concentrations of Benzaldehyde, ranging from 10% (93 mM) to $10^{-7}\%$. N = 9 locusts, n = 17 antennae, 50 repetitions. (B) Response profiles to different concentrations of Geraniol; 15% (93 mM), 25%, 50%, 75%, 100%. N = 4 locust, n = 6 antennae, 18 repetitions. In both A and B darker shades indicate higher concentrations. The duration of the stimulus is shaded gray. (C) and (D) show dose-response curves (maximum signal amplitude per concentration) for Benzaldehyde (data from A) and Geraniol (data from B) respectively. The standard error of the mean (SEM) represents by vertical lines (E) Chromatographic peak area detected in GC-MS of benzaldehyde at different decimal dilutions absorbed by a SPME fiber. Red line indicates blank (mineral oil) measurement, and therefore the device detection threshold. The lowest dilution the GC-MS was able to detect was 10^{-3} . Both axes are in log₁₀-scale for a better display of the lower concentrations' measurements. (F) A confusion matrix calculated for three train-test sets. The train groups comprise seven different odorants in addition to Benzaldehyde at five different concentrations. The test groups contain Benzaldehyde only, also with a sixth concentration not performed for the train group, for each set. Test concentrations are 10^0 , 10^{-2} or 10^{-4} . The accuracy values are 41% for 979 samples; 40% for 986 samples; and 61% for 981 samples, for the three concentrations, respectively.

Solid Phase Microextraction (SPME) fiber in the same experimental setup used for the locust antenna and used GC-MS to measure its thermally desorbed compound (see *GC-MS in Methods section*). Using this method, we were able to estimate the amounts of a representative odor (benzaldehyde) introduced onto the antenna in a single stimulus (Suppl. Table 3). Benzaldehyde in different decimal dilutions was applied to the SPME fiber, demonstrating a dose-response behavior similar to that obtained with the locust antenna (Fig. 3A, B, Fig. S5B). However, the detection level of the SPME fiber was four orders of magnitude less sensitive than the locust antenna detection level (Fig. 3A & C vs. E). Using the dose-response curve equation (Fig. S5B) and assuming linearity, we can estimate the antenna sensitivity limit to 256 pg. This is equivalent to a sensitivity threshold concentration of ~ 0.028 ppb because the volume of each pulse of air was 9.17 ml (1100 ml/min wind flow with a 0.5 s duration).

One of the main challenges of odor discrimination is that of the concentration invariance. Consequently, we next sought to test the bio-hybrid platform's ability to discriminate odors independently of their concentration.

Qualitatively scrutinizing the dose-response relative concentrations graphs suggests that the shape of the EAG signal is affected more by the odorant's identity than by its concentration (Fig. 2A and B, 3A,B & S6A). To confirm this observation using the random forest classifier, we divided the data into a test group, which contained repetitions of one concentration of Benzaldehyde, and a train group containing all other concentrations, together with the rest of the odorants. The classifier was still able to discriminate benzaldehyde from the other odorants at a concentration of $10^{-4}\%$, far above chance level, with a balanced accuracy of 53.85% even though it had never been exposed to this

concentration during training (compared to 12.5% random probability, $P < 0.0001$) (Fig. 3F). Testing the algorithm on higher concentrations led to similar results. (Fig. 3F, both $P < 0.0001$).

Last, we tested the platform's ability to discriminate the same odorant at different relative concentrations. Although the differences between the curves at different concentrations are minor (Fig. S6A), the classifier, using a 'Leave-one-group-out' paradigm, was again able to discriminate between six different concentrations of benzaldehyde at a 42.6% accuracy (random probability: 16.67%, Fig. S6B, $P < 0.0001$). These findings strengthen the uniqueness of this platform, as EAG is commonly very limited in its ability to determine an odorant's relative concentration.

3.3. Mixture of odors

As the world around us rarely contains only a single type of odor, we tested our platform's ability to identify odorants within mixtures of odorants. The Euclidean distances between the normalized graph of odorant responses (Fig. 4A, S7A) were used to select two pairs of odorants to be tested: (1) a relatively distant pair ((Benzaldehyde and β -Citronellol) (Fig. 4B, S7B)); and (2) a relatively close pair ((1-Hexanol and Ethyl butyrate) (Fig. 4C, S7C)). As Fig. 4B & C demonstrates, the curves of the mixture resemble the curve of the most potent odor of the pair. Our classifier was able to discriminate all of the odorants and their mixture in both pairs. As expected, the "distant pair" was identified at higher accuracy (79.9%) compared to the "close pair" (71.8%) (Fig. 4D&E), while both values were significantly higher than chance (33%, $P < 0.0001$).

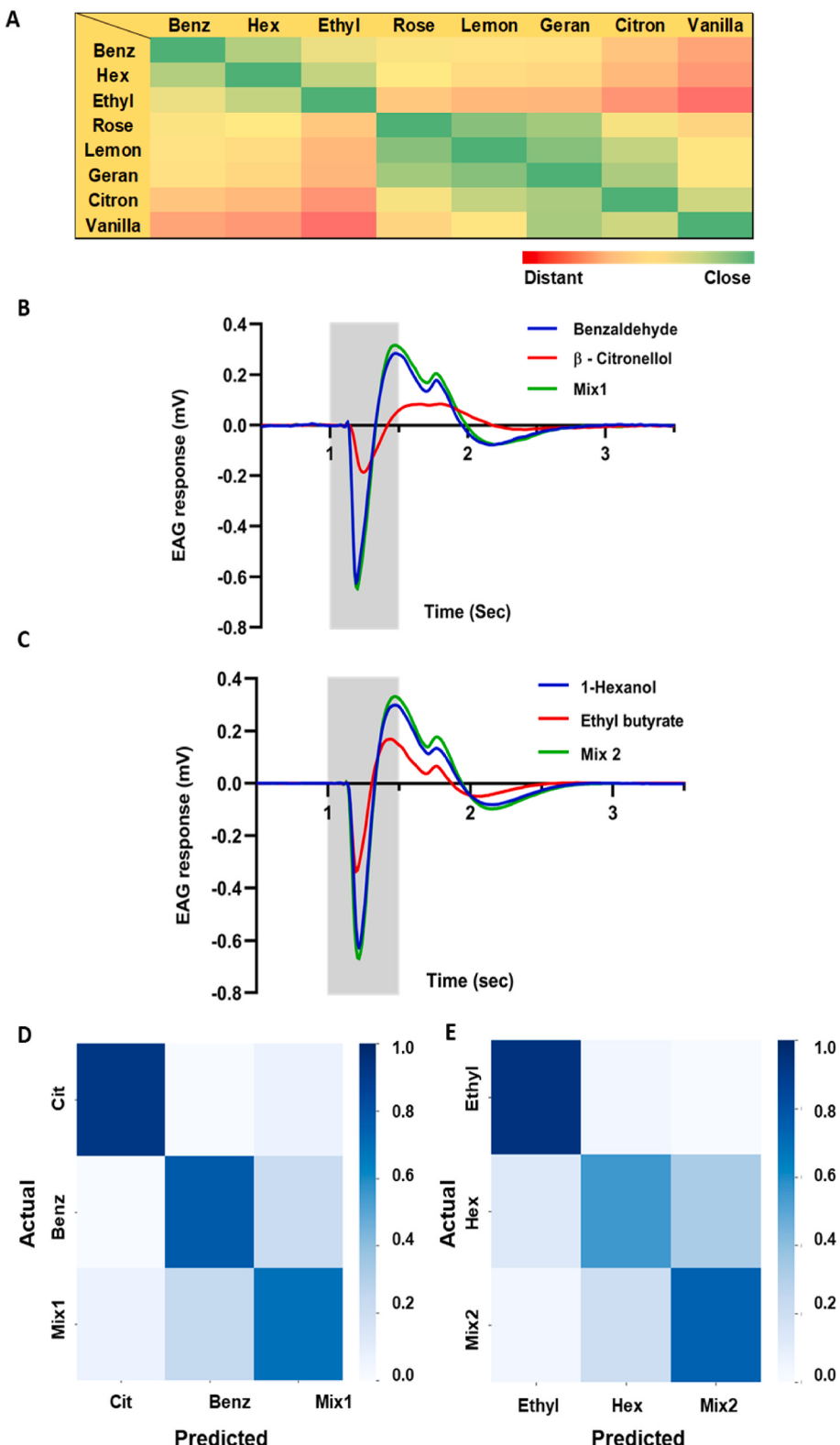


Fig. 4. The discrimination capacity of odors in a mixture. (A) Euclidean distances between the odorants based on the normalized data shown in Fig. 2B. Distance indicates less similarity in odors in contrast to Close, which indicates a greater similarity in odors. (B) Locust antennal responses to two distinct odors: Benzaldehyde, β -Citronellol, and their Mixture. N = 13 Locusts, n = 22–24 antennae, ~72 repetitions. (C) Locust antennal responses to two approximate odors: 1-Hexanol, Ethyl butyrate, and their Mixture. N = 20 Locusts, n = 38 antennae, 114 repetitions. In both B and C, the duration of the stimulus is shaded gray. (D) Confusion matrix for the odorants in A. 79.37% accuracy for 349 samples. (E) Confusion matrix for the odorants in B. 73.37% accuracy for 383 samples.

3.4. Antennal spatial and temporal sensing properties

We next sought to examine spatial differences within the locust antenna. Specifically, we examined the tentative role of the uneven distribution of olfactory receptors (Ochieng et al., 1998) and diverse firing patterns of the ORNs (Raman et al., 2010) in shaping the odor dependent EAG profile. To do so, after measuring the electrophysiological response

of the entire antenna, it was cut in half, the two halves were placed in special holders (similar to Fig. S1D but with a smaller gap), and their responses to the same odorant were examined (Fig. 5A). As shown in Fig. 5B&C, there were significant differences between the proximal vs. distal halves. It can be seen that the EAG amplitude is smaller in the proximal half than in the distal half, which might be due to fewer receptors in the former (Ochieng et al., 1998) (Fig. 5B&C). Moreover, after

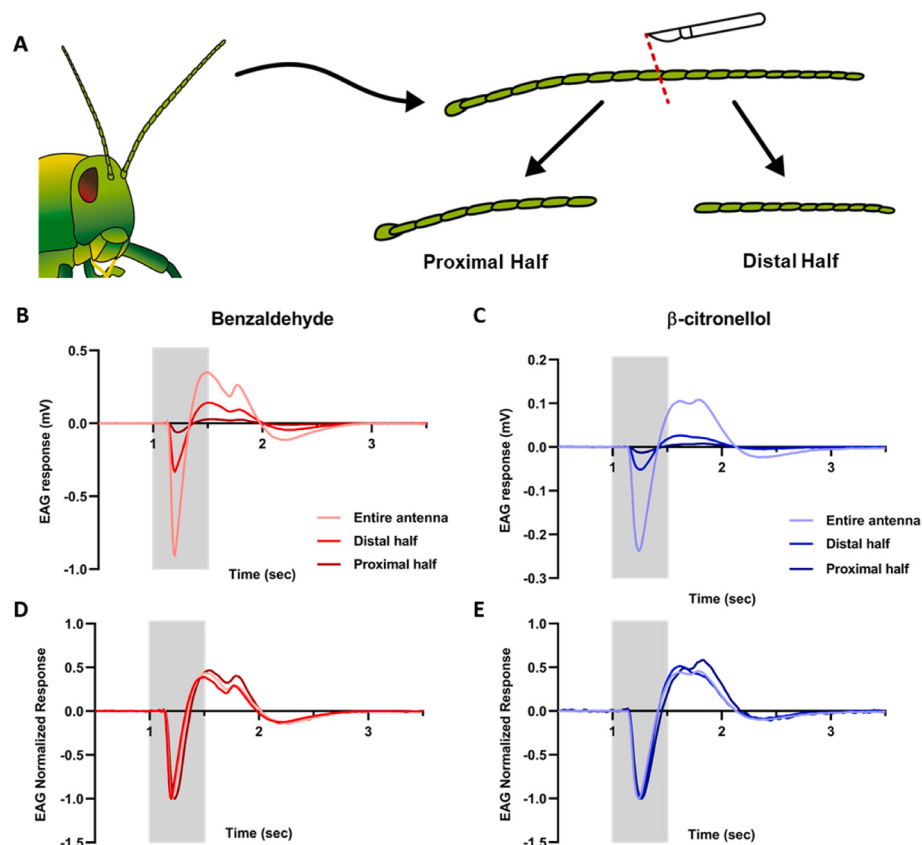


Fig. 5. Characterization of the response of different parts of the locust antenna. (A) Testing the entire antenna vs. the distal or proximal half. Response profiles to Benzaldehyde (B)&(D) and β -citronellol (C)&(E). N = 7 locusts, n = 13 antennae, 39 repetitions. (D) and (E) show the response profiles from B and C, respectively, with the most negative point normalized to -1. In B-E the duration of the stimulus is marked by a gray bar.

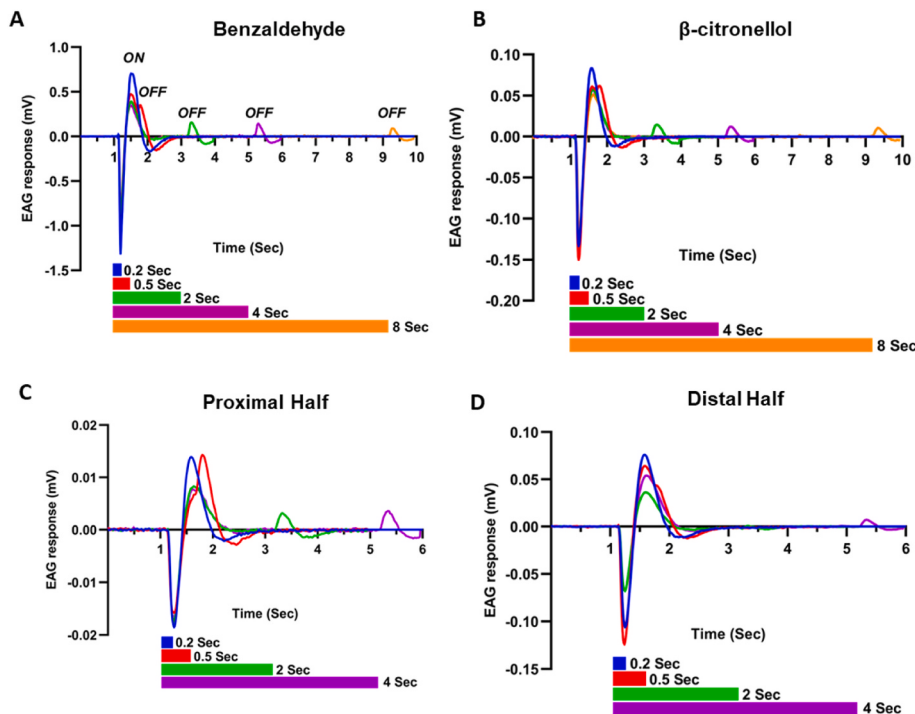


Fig. 6. Antenna response profile to different stimulus durations. (A) Benzaldehyde. N = 5 locusts, n = 9 antennae, 24 repetitions. and (B) β -citronellol. N = 7 locusts, n = 12 antennae, 36 repetitions. (C) and (D) show the response profile of the proximal (C) and distal (D) antenna halves to different durations of exposure to β -citronellol. N = 4 locusts, n = 7 antennae, 21 repetitions.

the curves were normalized, while for benzaldehyde the curve shape did not change significantly (Fig. 5D), the curve shape for β -citronellol visibly differed between the two parts (Fig. 5E). Furthermore, for both tested odors we could identify changes in the response kinetics, revealing that the *proximal* half seemingly has a delayed response compared to the *distal* one (Fig. 5D&E).

We next examined whether the stimulus duration affects the EAG response. As seen in Fig. 6A&B, there is a distinct ON-OFF response to the odorant application for both Benzaldehyde and β -Citronellol. We used the same experimental set-up as previously described in Fig. 5A (*proximal* vs. *distal*) and assessed how the different halves responded to different stimuli durations of β -citronellol (Fig. 6C&D). The 500 ms β -citronellol stimulus duration reproduced the results presented in Fig. 5C&E, i.e., the *proximal* half response was characterized by two positive voltage peaks: a low peak followed by a higher one; the *distal* half was characterized by a high positive peak followed by a lower one. A shorter stimulus duration caused these two, ON-OFF peaks, to consolidate into a single higher peak (Fig. 6C&D). For longer stimulus durations, the second peak, that is, the OFF peak, almost vanished for the *distal* half (Fig. 6D), while still appearing in the *proximal* half's response (Fig. 6C).

4. Discussion

We present a bio-hybrid discriminator, in which a biological sensory organ – the locust antenna – generates distinct electrical signals that are dependent on the specific response of olfactory receptor neurons- ORNs to air-borne odorants. We utilize the locust olfactory system, which offers several advantages: i.e., locusts are easy to breed, handle, and record from; they have been well studied and described; and they respond to a large variety of chemical odorant (probably due to the locust being an omnivorous insect). The biosensor we have developed displays enhanced sensitivity compared to the gas chromatograph-mass spectrometer, one of the most powerful and sensitive instruments for gas phase substance identification and quantitative determination that exists today (Fialkov et al., 2007). The successful identification by our system of all tested odorants, when presented individually, in different concentrations, as well as in mixtures, validates our approach, supporting further development and utilization of the system in simple and sturdy bio-hybrid robotic devices for various applications.

The odor-unique electrophysiological response of the antenna depends on the way that different types of ORNs respond to the stimulus. A recent study by (Nizampatnam et al., 2021) used antennal lobe (AL) recordings to identify two groups of olfactory neurons. One group of neurons was shown to fire as soon as the stimulus was applied and then continued to fire during the stimulation ('ON Neurons'), and the other group fired after the stimulus had ended ('OFF neurons'). They concluded that the locust's identification of the odor is influenced more by the ON-OFF neuron combination than by their firing pattern and rate. Our findings reconfirm this concept at the EAG level. It seems that the distinct EAG signals we record are created by a combination of 'ON-OFF' responses; and, moreover, as our findings suggest, by the spatial distribution of the different neuronal types along the antenna (in the proximal vs. distal parts of the antenna). A similar significant effect was found for the stimuli duration, in which intermediate-length stimuli, which partially combined the ON and OFF responses, produced the most complex EAG signal.

Previous studies have implied that the electroantennogram, which reflects the summed activity of all antennal ORNs, is not sufficient for odorant discrimination (Myrick et al., 2009; Park, 2002). Indeed, the EAG signals presented in the current work somewhat differ from those often described in the literature as comprising a single, simple curve shape (Ep-a et al., 2007; Van Der Pers and Minks, 1998). We believe that several factors enabled us to obtain more complex, information rich EAG signals: (1) The current study utilized a slightly higher HPF in comparison to previous studies (1 Hz vs. 0.1 Hz (Beck et al., 2012; Myrick et al.,

2008; Terutsuki et al., 2021)), allowing us to remove low frequency drifts. Our signals thus took a two-peak waveform shape (one negative peak, the other – positive and more complex), which did not exist in previous studies. (2) A standard stimulus duration (500 ms) was used in the current study, resulting in the two ON and OFF peaks partially overlapping, whereas longer stimulus durations caused the two peaks to separate at the beginning and end of the stimulation. (3) We utilized a custom-made, 3D printed antenna holder, interfacing the antenna and the recording electrodes via conductive gel-filled chambers. This enables EAG recordings without actual contact between electrodes and antenna, thereby resulting in a significantly high signal-to-noise ratio (S/N), revealing further details of the distinct odorant-induced responses, and allowing better signal identification. Overall, we note that the electrical signals obtained in the current study provided us with sufficient discriminatory information to enable consistent and robust odor identification and discrimination by way of the developed machine-learning algorithm. The algorithm, although considered a relatively simple learning method for classification, was robust enough to discriminate among mixtures of odors, and at different relative concentrations. The latter result is especially interesting, as it is extremely challenging to use EAG to identify relative concentrations.

To date, odor discrimination has only been performed using AL neuron spike recordings (Saha et al., 2020, 2017), by comparing multiple antennal responses in various insect species (Myrick et al., 2008; Park, 2002), or by means of temporal patterns obtained in single sensillum recordings from the ORNs (Raman et al., 2010). These methods require a highly skilled operator, sophisticated equipment, and complicated data analysis, compared to the discriminator proposed in this study. AL recordings for the purpose of discrimination have the drawback of variability in electrode positions between recordings. As a result of this inconsistency, researchers are forced to train locusts *de-novo* on the desired odor panel before performing the discrimination. Unlike AL recordings, EAG recordings remain consistent for a certain odor (applied under the same conditions) due to their nature of summing responses from antenna ORNs. Therefore, when using our method for discrimination, following the initial algorithm training there is no need to re-train each locust before each new recording.

5. Conclusions

We have presented a bio-hybrid odor identification and discrimination system based on an isolated *ex-vivo* locust antenna, improved EAG technology, and machine-learning algorithms. In order to be applicable in the real world (e.g., for locating and identifying malignant compounds, etc.), the technology developed and presented here still needs to overcome several important challenges. First, in the real world, odorants are generally not presented in isolation but, rather, in the presence of other interfering odors. Additionally, odors in nature exist in a wider range of concentrations, which can greatly affect their identification. Lastly, the algorithm appears to be stimuli-duration dependent. This, under realistic conditions in which the stimulus does not appear for a fixed period, may make identifying it more challenging. While there is still a long way to go, our findings provide important insights into the capacity of the system to meet these challenges. We have demonstrated that the concentration of the odorant presented is (to a large extent) immaterial to its identification and, moreover, the system was successful in olfactory discrimination when presented with different mixtures of odorants. A possible solution to the last challenge may be to construct a mechanism that will limit the stimulus exposure time, e.g., by inhaling a certain amount of air, or, alternatively, to train the algorithm on a 'train' set containing variable stimulus durations.

Our findings demonstrate the practicality of our approach and present great promise for the development of robotic devices with olfactory capabilities for various real-world applications.

Funding

This work was supported by the Israeli Ministry of Science, Technology and Space and by MAFAT.

CRediT authorship contribution statement

Shvil Neta: Writing – review & editing, Methodology, and, Formal analysis. **Golan Ariel:** Formal analysis. **Yovel Yossi:** Conceptualization, Supervision, Writing – review & editing. **Ayali Amir:** Conceptualization, Supervision, Writing – review & editing. **Maoz M. Ben:** Conceptualization, Supervision, Writing – review & editing.

Declaration of competing interest

The authors declare that they have no known competing financial interests or personal relationships that could have appeared to influence the work reported in this paper.

Data availability

Data will be made available on request.

Acknowledgments

We thank Ms. Yifat Weiss and Mr. Eyal Rosenfeld for their help in writing the code for EAG analysis, Dr. Anton Sheinin for his advice regarding building the EAG system. Dr. Daniel Knebel for his advice regarding the statistical tests and Dr. Alexander Gordin on his help with GC-MS experiment and data analysis.

Appendix A. Supplementary data

Supplementary data to this article can be found online at <https://doi.org/10.1016/j.bios.2022.114919>.

References

- Beck, J.J., Light, D.M., Gee, W.S., 2012. Electroantennographic bioassay as a screening tool for host plant volatiles. *JoVE*. <https://doi.org/10.3791/3931>.
- Chen, H., Huo, D., Zhang, J., 2022. Gas recognition in E-nose system: a review. *IEEE Trans Biomed Circuits Syst* 16, 169–184. <https://doi.org/10.1109/TBCAS.2022.31166530>.
- Ep-a, S., Bv, O.T.B.G., Technologies, X., Twente, U., Wo-a, B., Nv, K.K.P.N., Ep-a, P., Bv, Q.G., Bv, A.R., Delft, T.U., Chemistry, I., Ep-a, B., Nutricia, N.V., Agrotechnologie, W.U., Energieonderzoek, S., Nederland, C., 2007. A Practical Introduction . . . 052.
- Fialkov, A.B., Steiner, U., Lehota, S.J., Amirav, A., 2007. Sensitivity and noise in GC-MS: achieving low limits of detection for difficult analytes. *Int. J. Mass Spectrom.* 260, 31–48. <https://doi.org/10.1016/j.ijms.2006.07.002>.
- Fishel, I., Amit, Y., Shvil, N., Sheinin, A., Ayali, A., Yovel, Y., Maoz, B.M., 2021. Ear-bot: locust ear-on-a-chip bio-hybrid platform. *Sensors* 21, 1–11. <https://doi.org/10.3390/S21010228>.
- Hallem, E.A., Carlson, J.R., 2006. Coding of odors by a receptor repertoire. *Cell* 125, 143–160. <https://doi.org/10.1016/j.cell.2006.01.050>.
- Haney, S., Saha, D., Raman, B., Bazhenov, M., 2018. Differential effects of adaptation on odor discrimination. *J. Neurophysiol.* 120, 171–185. <https://doi.org/10.1152/jn.00389.2017>.
- Jacob, V.E.J.M., 2018. Current source density analysis of electroantennogram recordings – a tool for mapping the olfactory response in an insect antenna. *Front. Cell. Neurosci.* 12, 1–19. <https://doi.org/10.3389/fncel.2018.00287>.
- Kaissling, K.E., Priesner, E., 1970. Die Riechschwelle des Seidenspinners. *Naturwissenschaften* 57 (1 57), 23–28. <https://doi.org/10.1007/BF00593550>, 1970.
- Kuwana, Y., Nagasawa, S., Shimoyama, I., Kanazaki, R., 1999. Synthesis of the pheromone-oriented behaviour of silkworm moths by a mobile robot with moth antennae as pheromone sensors. *Biosens. Bioelectron.* 14, 195–202. [https://doi.org/10.1016/S0956-5663\(98\)00106-7](https://doi.org/10.1016/S0956-5663(98)00106-7).
- Larisika, M., Kotlowski, C., Steininger, C., Mastrogiamico, R., Pelosi, P., Schütz, S., Petru, S.F., Kleber, C., Reiner-Rozman, C., Nowak, C., Knoll, W., 2015. Electronic olfactory sensor based on *A. mellifera* odorant-binding protein 14 on a reduced graphene oxide field-effect transistor. *Angew. Chem.* 127, 13443–13446. <https://doi.org/10.1002/ANGE.201505712>.
- Latif, T., Whitmire, E., Novak, T., Bozkurt, A., 2016. Sound localization sensors for search and rescue biobots. *IEEE Sensor. J.* 16, 3444–3453. <https://doi.org/10.1109/JSEN.2015.2477443>.
- Lockey, J.K., Willis, M.A., 2015. One antenna, two antennae, big antennae, small: total antennae length, not bilateral symmetry, predicts odor-tracking performance in the American cockroach *Periplaneta americana*. *J. Exp. Biol.* 218, 2156–2165. <https://doi.org/10.1242/jeb.117721>.
- Mallik, S., Nizampatnam, S., Nandi, A., Saha, D., Raman, B., Ching, S., 2020. Neural circuit dynamics for sensory detection. *The Journal of Neuroscience JN-RM-2185-19*. <https://doi.org/10.1523/jneurosci.2185-19.2020>.
- Martinez, D., Arhidi, L., Demondion, E., Masson, J.B., Lucas, P., 2014. Using insect electroantennogram sensors on autonomous robots for Olfactory searches. *JoVE* 1–9. <https://doi.org/10.3791/51704>.
- Myrick, A.J., Park, K.C., Hetling, J.R., Baker, T.C., 2009. Detection and discrimination of mixed odor strands in overlapping plumes using an insect-antenna-based chemosensor system. *J. Chem. Ecol.* 35, 118–130. <https://doi.org/10.1007/s10886-008-9582-4>.
- Myrick, A.J., Park, K.C., Hetling, J.R., Baker, T.C., 2008. Real-time odor discrimination using a bioelectronic sensor array based on the insect electroantennogram. *Bioinspiration Biomimetics* 3. <https://doi.org/10.1088/1748-3182/3/4/046006>.
- Nakhleh, M.K., Amal, H., Jeries, R., Broza, Y.Y., Aboud, M., Gharra, A., Ivgi, H., Khatib, S., Badarneh, S., Har-Shai, L., Glass-Marmor, L., Lejbkowicz, I., Miller, A., Badarny, S., Winer, R., Finberg, J., Cohen-Kaminsky, S., Perros, F., Montani, D., Girerd, B., Garcia, G., Simonneau, G., Nakhoul, F., Baram, S., Salim, R., Hakim, M., Gruber, M., Ronen, O., Marshak, T., Doweck, I., Nativ, O., Bahouth, Z., Shi, D.Y., Zhang, W., Hua, Q.L., Pan, Y.Y., Tao, L., Liu, H., Karban, A., Koifman, E., Rainis, T., Skapars, R., Sivins, A., Ancans, G., Liepniece-Karele, I., Kikuste, I., Lasina, I., Tolmanis, I., Johnson, D., Millstone, S.Z., Fulton, J., Wells, J.W., Wilf, L.H., Humbert, M., Leja, M., Peled, N., Haick, H., 2017. Diagnosis and classification of 17 diseases from 1404 subjects via pattern analysis of exhaled molecules. *ACS Nano* 11, 112–125. <https://doi.org/10.1021/acsnano.6b04930>.
- Nizampatnam, S., Saha, D., Chandak, R., Raman, B., 2018. Dynamic contrast enhancement and flexible odor codes. *Nat. Commun.* 9 <https://doi.org/10.1038/s41467-018-05533-6>.
- Nizampatnam, S., Zhang, L., Chandak, R., Li, J., Raman, B., Hildebrand, J., 2021. Invariant Odor Recognition with ON-OFF Neural Ensembles. <https://doi.org/10.1073/pnas.2023340118/-DCSupplemental>.
- Ochieng, S.A., Hallberg, E., Hansson, B.S., 1998. Fine structure and distribution of antennal sensilla of the desert locust, *Schistocerca gregaria* (Orthoptera: acrididae). *Cell Tissue Res.* 291 (3 291), 525–536. <https://doi.org/10.1007/S004410051022>, 1998.
- Olsson, S.B., Hansson, B.S., 2013. Electroantennogram and single sensillum recording in insect antennae. *Methods Mol. Biol.* 1068, 157–177. https://doi.org/10.1007/978-1-62703-619-1_11.
- Park, K.C., 2002. Odor discrimination using insect electroantennogram responses from an insect antennal array. *Chem. Senses* 27, 343–352. <https://doi.org/10.1093/chemse/27.4.343>.
- Raman, B., Joseph, J., Tang, J., Stopfer, M., 2010. Behavioral/Systems/Cognitive Temporally Diverse Firing Patterns in Olfactory Receptor Neurons Underlie Spatiotemporal Neural Codes for Odors. <https://doi.org/10.1523/JNEUROSCI.5639-09.2010>.
- Renou, M., Anton, S., 2020. Insect olfactory communication in a complex and changing world. *Current Opinion in Insect Science*. <https://doi.org/10.1016/j.cois.2020.04.004>.
- Rogers, L.J., Rigosi, E., Frasnelli, E., Vallortigara, G., 2013. A right antenna for social behaviour in honeybees. *Sci. Rep.* 3, 1–4. <https://doi.org/10.1038/srep02045>.
- Saha, D., Leong, K., Katta, N., Raman, B., 2013a. Multi-unit recording methods to characterize neural activity in the locust (*Schistocerca americana*) olfactory circuits. *JoVE : JOVE 1–10*. <https://doi.org/10.3791/50139>.
- Saha, D., Leong, K., Li, C., Peterson, S., Siegel, G., Raman, B., 2013b. A spatiotemporal coding mechanism for background-invariant odor recognition. *Nat. Neurosci.* 16, 1830–1839. <https://doi.org/10.1038/nn.3570>.
- Saha, D., Mehta, D., Altan, E., Chandak, R., Traner, M., Lo, R., Gupta, P., Singamaneni, S., Chakrabarty, S., Raman, B., 2020. Explosive sensing with insect-based biorobots. *Biosens. Bioelectron.* X 6, 1–28. <https://doi.org/10.1016/j.biosx.2020.100050>.
- Saha, D., Sun, W., Li, C., Nizampatnam, S., Padovano, W., Chen, Z., Chen, A., Altan, E., Lo, R., Barbour, D.L., Raman, B., 2017. Engaging and disengaging recurrent inhibition coincides with sensing and unsensing of a sensory stimulus. *Nat. Commun.* 8, 1–19. <https://doi.org/10.1038/ncomms15413>.
- Shor, E., Herrero-Vidal, P., Dewan, A., Uguz, I., Curto, V., Malliaras, G., Savin, C., Bozza, T., Rinberg, D., 2020. A Mouse Bio-Electronic Nose for Sensitive and Versatile Chemical Detection. <https://doi.org/10.1101/2020.05.06.079772>.
- Skarysz, A., Alkhalfah, Y., Darnley, K., Eddleston, M., Hu, Y., McLaren, D.B., Nailon, W. H., Salman, D., Sykora, M., Thomas, C.L.P., Soltoggio, A., 2018. Convolutional neural networks for automated targeted analysis of raw gas chromatography-mass spectrometry data. *Proceedings of the International Joint Conference on Neural Networks*. <https://doi.org/10.1109/IJCNN.2018.8489539>, 2018-July.
- Terutski, D., Uchida, T., Fukui, C., Stukewawa, Y., Okamoto, Y., Kanazaki, R., 2021. Real-time odor concentration and direction recognition for efficient odor source localization using a small bio-hybrid drone. *Sens. Actuators, B* 339, 129770. <https://doi.org/10.1016/j.snb.2021.129770>.
- Van Der Pers, J.N.C., Minks, A.K., 1998. A portable electroantennogram sensor for routine measurements of pheromone concentrations in greenhouses. *Entomol. Exp. Appl.* 87, 209–215. <https://doi.org/10.1046/j.1570-7458.1998.00322.x>.
- Vouloutsi, V., Lopez-Serrano, L.L., Mathews, Z., Chimeno, A.E., Ziyatdinov, A., Perera i Lluna, A., Bermúdez i Badia, S., Verschure, P.F.M.J., 2015. The synthetic moth: a

neuromorphic approach toward artificial olfaction in robots. *Neuromorphic Olfaction* 117–152. <https://doi.org/10.1201/b14670-9>.